Available online at www.sciencedirect.com
ScienceDirect
Journal of Photochemistry and Photobiology A: Chemistry 189 (2007) 239–246
Journal of Photochemistry and Photobiology A:Chemistry
www.elsevier.com/locate/jphotochem

# Effects of experimental conditions on *E. coli* survival during solar photocatalytic water disinfection

Cosima Sichel, Julián Blanco, Sixto Malato, Pilar Fernández-Ibáñez *

*Plataforma Solar de Almería, CIEMAT, P.O. Box 22, 04200 Tabernas, Almería, Spain*

Received 4 October 2006; received in revised form 2 February 2007; accepted 5 February 2007
Available online 11 February 2007

**Abstract**

Results of photocatalytic disinfection of *Escherichia coli* K12 in water in a compound parabolic collector (CPC) solar reactor are reported. The aim of the study is to quantify the influence of operating parameters, such as flow rate, water quality and bacterial concentration, on bacterial viability in solar photocatalysis and in the dark. The catalyst used was an industrial titanium-dioxide-coated paper matrix fixed on a tubular support in the focus of the CPC. Addition of $TiO_2$ notably improved solar-only disinfection up to 6 logs disinfection in 90 min. Between 10 and 2 L/min, photocatalytic disinfection effectiveness tended to increase with decreasing flow rates.

In dark experiments, inactivation of 99% of viable *E. coli* cells in distilled water was detected after 90 min of recirculation at 10 L/min in the CPC reactor. A detailed study of bacterial viability in the solar reactor in the dark was therefore performed, varying flow rates, initial concentrations and osmolarity. It was found that bacterial viability in the reactor strongly depends on all the parameters examined, so that disinfection and dark inactivation overlap when working under low-osmolarity conditions and low bacterial concentrations.


*Keywords:* Osmotic stress; Mechanical stress; Solar reactor; Photocatalytic disinfection; *E. coli*

## 1. Introduction

A growing number of countries around the world have irrigation and drinking water supply problems. Many water sources are not only polluted by hazardous chemicals but also by pathogenic microorganisms and therefore, have to be disinfected before use. The most commonly used techniques for water disinfection are chlorination, heating and ozonation. The negative effect of chlorination is the appearance of trihalomethanes (THMs) as by products of its reaction with organic matter. It also gives drinking water an unpleasant taste [1,2]. When used for irrigation, chlorine is often phytotoxic [3]. Other methods, e.g., ozonation, are either moderately expensive or involve high consumption of energy that is usually not sustainably produced [1].

Often countries with the most serious safe water supply problems are among the sunniest in the world. This is why solar water disinfection methods for mainly rural areas, such as a special solar drinking-water disinfection process called SODIS, have gained support in recent years. SODIS can be used as a sustainable small-scale, low-cost water treatment in transparent plastic bottles, and has been proven successful for the disinfection of a wide range of microorganisms [4,5]. SODIS bases on the pasteurizing effect of solar radiation at temperatures higher than 40–45 °C and on the synergistic interaction between the elevated temperatures and solar irradiation [6,7]. Moreover, in some water matrixes sunlight can produce highly reactive oxygen species which attack bacterial cells and contribute to their inactivation [8,9]. Nevertheless, disinfection efficacy of the SODIS treatment can easily be affected by water turbidity, low irradiation intensity and regrowth of bacteria after the solar treatment, probably due to photo-repair mechanisms [8–10].

On the other hand, heterogeneous photocatalysis with $TiO_2$, one of the new "Advanced Oxidation Technologies" (AOT), is a "clean", low-cost water treatment technology which can offer additional advantages in a wide range of applications [11]. These technologies are based on the production of $OH^{\bullet}$ radicals, and as they do not require the addition of chemical consumables, do not produce hazardous waste products. When the catalytic semiconductor $TiO_2$ is photoexcited with UV light at a wavelength equal

* Corresponding author. Tel.: +34 950387957; fax: +34 950365015.
*E-mail address:* pilar.fernandez@psa.es (P. Fernández-Ibáñez).

1010-6030/$ – see front matter © 2007 Elsevier B.V. All rights reserved.
doi:10.1016/j.jphotochem.2007.02.004

to or lower than 390 nm, electron hole pairs are generated. In the presence of water and dissolved oxygen, hydroxyl radicals, which are very reactive and have a short lifetime, can be generated [12]. Photocatalytic disinfection has been demonstrated to be mainly controlled by temperature, catalyst physicochemical properties and concentration, microorganism type and concentration, light intensity, exposure time and whether radiation is natural or simulated [11].

Application of $TiO_2$ to water treatment has been reviewed by Fujishima et al. [13] and more recently by Herrmann [11]. In recent years, scientific and engineering interest in $TiO_2$, especially photocatalysis for disinfection, has grown exponentially [9,14–17]. Its wide field of application has been reviewed by Blake et al. [18]. Some authors suggest that the cell membrane is the primary site of attack by the reactive hydroxyl radicals [19,20]. Maness reported results that can be explained by peroxidation of the polyunsaturated phospholipid component of the lipid cell membrane leading to a loss of essential cell functions, e.g., respiratory activity, and in the end, to cell death. Most work has been done with $TiO_2$ powder in a slurry, some of it under natural sunlight, because reaction yields are better [21,22]. Disinfection with supported $TiO_2$ has reduced the need of post-treatment not only in the laboratory, but also in large solar reactors [8,15,23].

Different types of solar photocatalytic and solar-only disinfection reactor configurations have been tested with promising results [24–26]. Compound parabolic reactors (CPCs) have been found to be very effective for treatment of water polluted by chemicals as well as for disinfection [23,26,27]. Photocatalytic disinfection in solar reactors is the last step in research before application to final disinfection systems, therefore optimisation of the disinfection yield and suitability of the treated water for its final use are major concerns at this stage of development. In many applications, rigorous study of photocatalytic disinfection requires the treatment water to have controlled chemical properties. Thus, the majority of work in this field uses artificially contaminated samples that are prepared with a standard microorganism in distilled water. With this medium, a significant negative affect on bacterial viability is not expected during various days [28]. Very little work has been done with real water sources, such as rivers, lakes and wells as reported by Rincón and Pulgarín [15] and Wist et al. [29].

This work starts out with the detrimental effect of agitation on bacterial viability found under specific experimental conditions (distilled water and low bacterial concentration) in solar photocatalytic reactors. The negative effects of water recirculation in solar reactors have not yet been described. Nevertheless, cell damage due to agitation has been studied in other processes [30–34]. Due to the very complex interrelationships of inactivation mechanisms during disinfection, factors not forming part of solar and solar photocatalytic inactivation mechanisms that coexist in the process are often underestimated. Since these parameters have been demonstrated to significantly affect disinfection results under certain conditions, correct evaluation of photocatalytic performance can be hindered. This clearly affects reactor efficiency evaluation and therefore subsequent optimisation of the disinfection system. In addition to identifying and measuring such parameters coexisting in the solar photocatalytic process, this work aims to set criteria for solar reactor operation protocols during optimization.

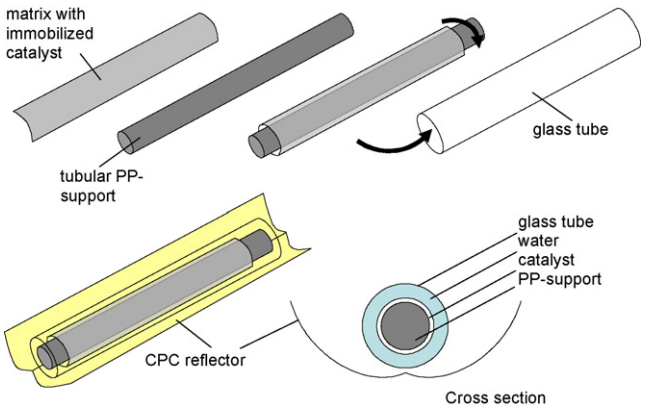


Fig. 1. Diagram of the catalyst arrangement in the CPC reactor.

## 2. Experimental methods

### 2.1. Solar CPC photoreactors

All the photocatalytic experiments were carried out under sunlight at the Plataforma Solar de Almería (Spain, local latitude 37°N, longitude 2.4°W) using compound parabolic solar collectors (CPC) fabricated by AOSOL Ltd. (Portugal) and installed in the experimental prototype manufactured by Ecosystem, Environmental Services, S.A. (Barcelona, Spain). All experiments were done in the morning on completely sunny days from May to July 2005. The photoreactor module used was designed and built expressly for a photocatalyst immobilized on tubular supports. The supports are inserted in two borosilicate glass tubes (Glass Type 3.3, Schott-Duran, Germany, cut-off at 280 nm) which are placed in the focus of CPC reflectors (Fig. 1) designed for the best optical performance under these particular conditions [35]. The systems (tubes + supports + CPC collectors) are held by aluminium frames mounted on platforms tilted 37° local latitude (Fig. 2). The glass tubes are connected so that water flows directly from one to another and finally into a tank (Fig. 2). A centrifugal pump (20 W, Panworld, Spain) then returns the water to the collectors. The tank has an aperture on top where the contaminated water can be poured in. For the disinfection process, this aperture is closed with a plastic lid. The treated water is

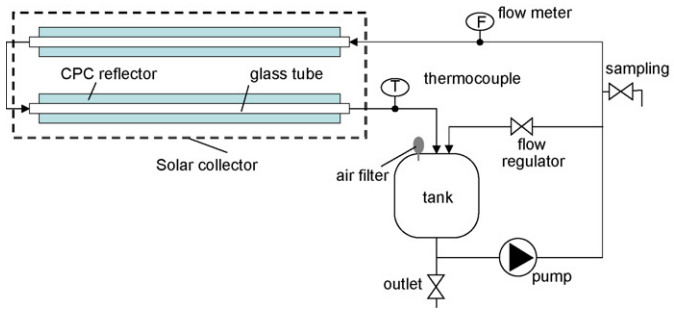


Fig. 2. Flow diagram of the solar CPC photoreactor.

later recovered by opening the outlet valve. Similar CPC photoreactors have previously been described in detail elsewhere [11,23,27,36]). The photoreactor volume is 14 L and the illuminated volume for the whole system is 2.27 L. The illuminated surface of the solar collector is 0.41 $m^2$. The outer diameter of the glass tubes is 50 mm.

### 2.2. Catalyst

Fixed-catalyst experiments were performed using a synthetic fibre support, Type KN "Ahlstrom paper"© (organic fibres, homogeneous weave, 460-μm thick and weight 80 g $m^{-2}$) manufactured by Ahlstrom Research & Services, France [37], and coated with Degussa P25 $TiO_2$ at a dose of 20 g $TiO_2$ $m^{-2}$ using an inorganic binder, an aqueous dispersion of colloidal $SiO_2$, which is transparent to UV radiation [37,38]. Sheets of the coated Ahlstrom paper were fastened on the concentric support and inserted in the CPC photo-reactor for photocatalytic experiments (Fig. 1). The Ahlstrom catalyst was washed several times following a specifically designed protocol (three runs with only distilled water) before its first use to rule out the possibility of material leaching into the water. No $TiO_2$ was detected in spectrometric measurements of the rinse water.

### 2.3. Evaluation of solar UV radiation

$Q_{UV}$ is used to interpret results in solar reactor systems. This magnitude estimates accumulated UV energy in the photoreactor per unit of treated water volume for given periods of time during the experiment. It is used to normalize the energy dose for the photocatalytic reaction in the CPC reactor. The intensity of solar UV radiation is measured by a global UV radiometer (Mod. CUV3, KIPP&ZONEN, the Netherlands) with a typical sensitivity of 264 μV/W/$m^2$ and a central wavelength of 300–400 nm, mounted on a platform tilted 37° (the same angle as the CPCs), which provides data in terms of incident $W_{UV}/m^2$. With this, the total UV energy received on any surface in the same position with regard to the sun is calculated per unit of volume in the reactor using Eq. (1) [39] where $t_n$ is the experimental time for $n$-sample, $\overline{UV}_{n-1}$ is the average solar ultraviolet radiation measured during the period $(t_n - t_{n-1})$, $A_r$ is the illuminated collector surface and $V_t$, the total reactor volume.

$$Q_{UV} = \sum_n \overline{UV}_{n-1} \frac{A_r}{V_t}(t_n - t_{n-1}) \quad (1)$$

Consequently, when $Q_{UV}$ is used, the reaction rate is expressed in terms of decrease in colony forming units (CFU) concentration per Jules of UV energy reaching the collector surface.

### 2.4. Bacterial strain and quantification

*Escherichia coli* K-12, ATCC 23631 was inoculated in a Luria Broth nutrient medium (Miller's LB Broth, Sigma–Aldrich, USA) and incubated at 37 °C with constant agitation on a rotary shaker at 100 rpm for 24 h. The stationary phase of bacterial growth yielded a concentration of $10^9$ CFU/mL. For all experiments, the range of initial concentrations ($C_0$) of *E. coli* was from $10^4$ to $10^7$ CFU/mL. For initial concentrations of $10^4$ CFU/mL, *E. coli* suspensions were prepared with distilled water directly in the photoreactor tank by inoculating 140 μL of a concentrated culture in 14 L of water. For higher concentrations, *E. coli* suspensions were centrifuged at 3000 rpm for 10 min and washed three times with saline solution (0.9% NaCl). Finally, the bacteria pellet was resuspended in distilled water and diluted in the 14-L tank to reach the required cell density. Samples were serially diluted in distilled water and plated. Every sample was plated 16 times (16 × 10 μL) on Luria agar (Sigma–Aldrich). The detection limit for this method of quantification is 6 CFU/mL. Inoculated samples were incubated at 37 °C for 24 h before counting.

### 2.5. CPC reactor experiments

"Dark runs" were performed under exactly the same photoreactor conditions as "solar $TiO_2$ photocatalysis" tests, but in the dark, by placing a black cover over the solar collectors. "Solar disinfection" experiments were carried out in the presence of sunlight without a catalyst, but with the catalyst support in the collector tubes. The bacteria suspension was prepared directly in the reactor using various *E. coli* concentrations. For homogenisation and to let bacteria adjust to the environment before exposure, the reactor was kept running in the dark for 15 min. The 0-min "control sample" was kept in the dark in a 15-mL tube at 20 °C and stirred slowly (100 rpm). After 90 min, this sample was re-plated at the same time as the 90-min reactor sample. For "saline solution" experiments, NaCl was added to the reactor water at 0.9 wt.% All the other experiments were done with distilled water. Although the temperature of the water in the reactor was not controlled, this parameter was monitored during all the experiments to avoid testing at over 36 °C. All experiments were repeated three times to ensure reproducibility of results. The results reported are the average of these three replicates. The error bars correspond to the statistical error of the 3 (replicates) × 16 (inoculations), i.e., a 95% confidence level.

### 2.6. Modelling with GinaFiT

The results from the photocatalytic experiments done with different initial bacterial concentrations were fitted to the Geeraed and Van Impe inactivation model, GinaFiT [40,41]. This model has been employed successfully to fit solar disinfection inactivation results by Barney et al. [7,42]. It admits six different types of microbial survival tests: log-linear regression [43], log-linear + tail [40], log-linear + shoulder [40], log-linear + shoulder + tail [40], Weibull model [44], biphasic model [45], and biphasic + shoulder model [41]. For each inactivation curve modelled, the fit result was the smallest root mean sum of squared errors (RSME). The RSME is considered by Geeraerd et al. [41] to be the most informative measure of the goodness of fit. Most of our results fit the log-linear regression + shoulder best. The $Q_{90}$ value was also used for comparison of inactivation curves; this parameter represents the accumulated UV energy ($Q_{UV}$) necessary to reduce the concentration

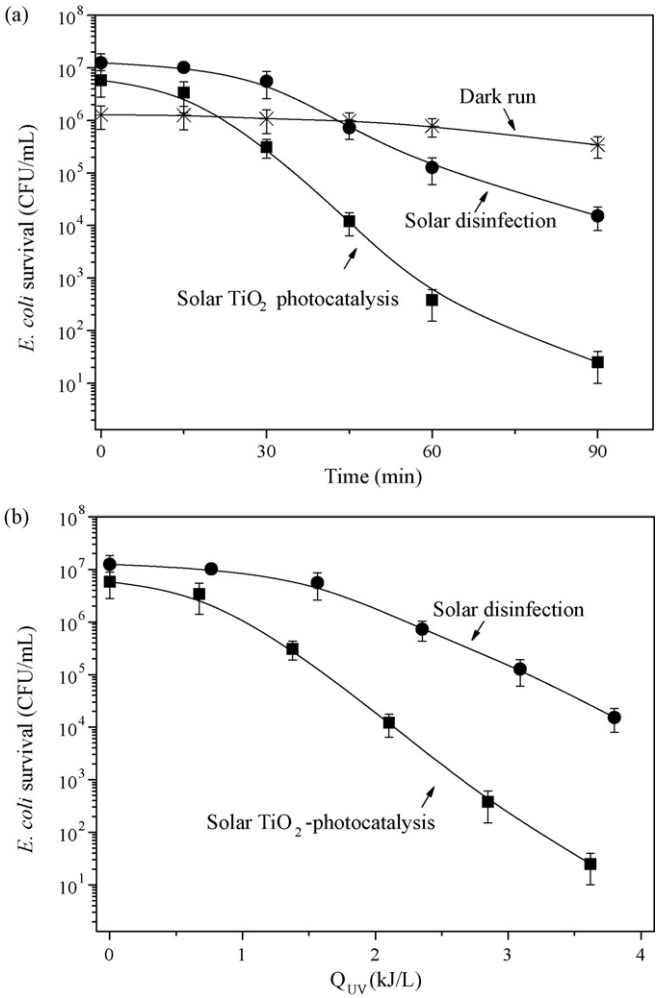


Fig. 3. (a) *E. coli* concentration in the CPC reactor during solar disinfection (●) and solar $TiO_2$ photocatalytic experiments (■) at an initial bacterial concentration of around $10^7$ CFU/mL. Dark run at $C_0 \sim 10^6$ CFU/mL (×). Distilled water flow rate 2 L/min. (b) *E. coli* concentration vs. $Q_{UV}$ for the same experiments, same symbols. Each point represents the average. The bars show the statistical error at a 95% level of confidence.

of viable bacteria by 90%. $Q_{90}$ was calculated on the basis of the GinaFiT model results.

## 3. Results and discussion

### 3.1. Solar photocatalysis at high bacterial concentrations

In spite of the fact that bacterial viability decreases slightly in the absence of ions, solar and solar photocatalytic experiments were done with distilled water to avoid interference of specific ions and organic compounds with the photocatalytic process. Since, as shown below, the osmotic effect is less important in high bacterial concentrations, the photocatalytic experiments were done at initial concentrations over $10^5$ CFU/mL. Above this concentration bacteria are still inactivated in the dark, but the photocatalytic result is not disturbed. The flow rate was 2 L/min for the experiments shown in Fig. 3.

Bacterial concentration in the dark ("dark run") are observed to remain almost stable throughout the experiment, while solar disinfection led to a 3-log decrease in concentration and the solar photocatalysis experiment 6-log. Both inactivation curves show a shoulder effect that can be seen in all the photocatalytic disinfection curves presented. Average UV irradiation received during the $TiO_2$ disinfection experiment was 22 W/m$^2$ for a solar dose of 119.5 kJ/m$^2$.

At high bacterial concentrations, photocatalytic disinfection was therefore clear. This 6-log disinfection after 90 min of solar photocatalytic treatment is very promising for fixed $TiO_2$ catalyst applications. Similar results have been found previously, but only in the laboratory [14] or in small-scale bottle reactors [8]. Rincón and Pulgarín reported a 5-log disinfection after 120–150 min exposure to irradiation with different-strength $TiO_2$ fixed catalysts using milli-Q water in bottle reactors (40 mL) and a solar simulator (400 W/m$^2$). In photocatalytic experiments under natural sunlight, disinfection of 11 L in CPC reactors with supported catalysts was only 2-log in 60 min [23].

The interest in using the Ahlstrom, or any other immobilised catalyst, is development of a solar photocatalytic disinfection system feasible for water treatment. The main advantage of using an immobilised catalyst is that it avoids the need to separate fine $TiO_2$ particles from the suspension after treatment.

### 3.2. Mechanical stress superimposed on photocatalytic effects

The series of experiments shown in Fig. 4 compares experiments in the dark with experiments under solar radiation. Initial bacterial concentrations for these experiments were about $10^4$ CFU/mL. An almost identical decrease in *E. coli* viability within the experimental error was observed in both runs. In both cases, the bacterial concentration reached the detection limit after 90 min. Any possible adsorption of bacterial cells on the catalyst surface has been dismissed, because identical results

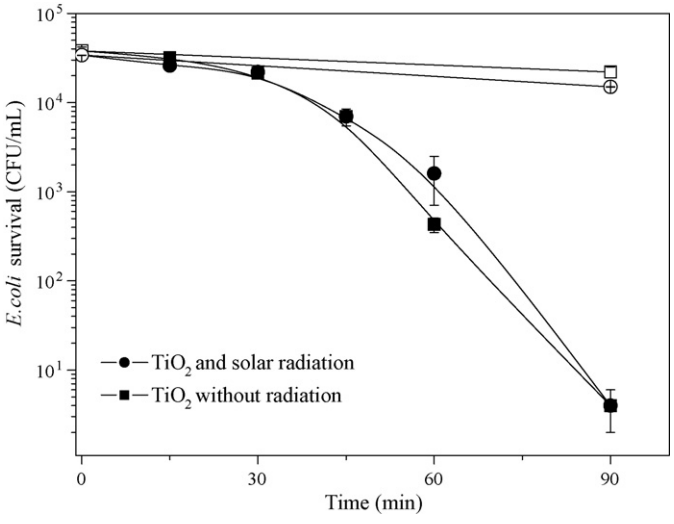


Fig. 4. *E. coli* concentration in the CPC reactor in the dark (■) and under solar radiation (●). Initial bacterial concentration $3 \times 10^4$ CFU/mL. Distilled water flow rate 10 L/min. Open symbols (□, ○) are control samples. Each point represents an average; the bars show the statistical error at a 95% level of confidence.

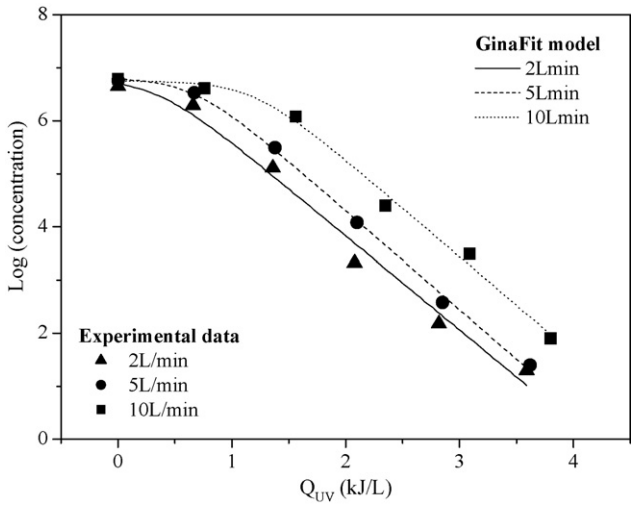


Fig. 5. *E. coli* concentration in the CPC reactor during solar $TiO_2$ photocatalytic experiments in distilled water at 10 L/min (■), 5 L/min (●), and 2 L/min (▲). $C_0 \sim 5 \times 10^6$ CFU/mL. Corresponding GinaFit model fits: log linear regression with shoulder.

were found during the "dark runs" without catalyst paper. These results show the strong impact that mechanical stress in the CPC reactors has on the viability of *E. coli* cells. Therefore, the effect of stress prevailing in the CPC reactor in the dark may be said to overlap with photocatalytic disinfection.

### 3.3. Influence of flow rate on photocatalytic disinfection

To study the effect of different flow rates on bacterial inactivation, a series of experiments was performed at 2, 5 and 10 L/min with the photocatalyst under sunlight (Fig. 5) and in the dark (Fig. 6). The best fits for the inactivation curves in Fig. 5 were obtained with GinaFiT for a log linear regression with shoulder. While the maximum reaction constants $k_{max}$ found in the fit are very similar ($k_{2\,L/min} = 4.08$, $k_{5\,L/min} = 4.29$, $k_{10\,L/min} = 4.2$), the shoulder, and therefore, $Q_{90}$, increases with increased flow

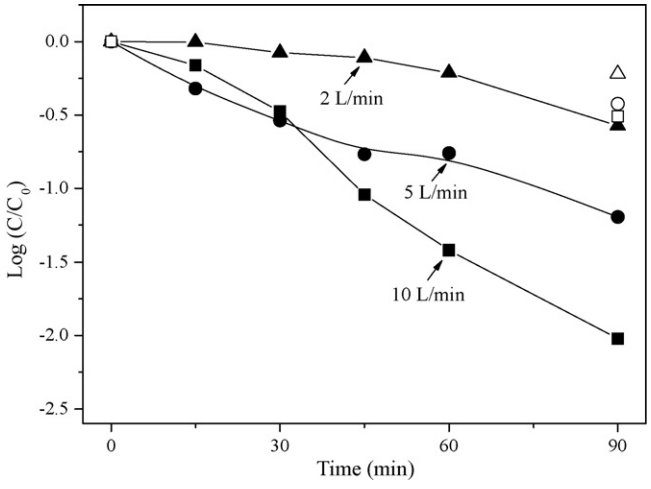


Fig. 6. *E. coli* concentration during dark runs at flow rates of 10 L/min (■), 5 L/min (●), and 2 L/min (▲). $C_0 \sim 10^6$ CFU/mL. Open symbols (□, ◯, △) are control samples. Each point is an average; the bars show the statistical error at a 95% level of confidence.

rate. At 2 L/min $Q_{90}$ is 0.72 kJ/L, at 5 L/min 0.98 kJ/L, and for 10 L/min 1.52 kJ/L. This increase in the shoulder, or lag, means that photocatalytic disinfection is less at higher flow rates than at lower.

While in a $TiO_2$ slurry dissolved oxygen can become a reaction constraint [16], higher flow rates in the reactor lead us to expect better disinfection efficiencies, especially when oxygen only enters by contact with the air from water recirculation. This was confirmed in our work on $TiO_2$ in slurry at flow rates of 5–22.5 L/min [23]. The main difference between fixed and slurry photocatalysis systems is the surface area of the catalyst, and therefore reaction yield and oxygen consumption are lower throughout the reaction. Consequently, it may be assumed that the main immobilised catalyst reaction constraint is the interaction between the catalyst surface and the target microorganism, not the oxygen supply. Agitation is not crucial for disinfection with fixed $TiO_2$ as shown by the very good disinfection results recently reported with fixed $TiO_2$ [8]. These authors demonstrated a 4-log decrease in faecal coliforms after 30 min irradiation in PET bottles with $TiO_2$ supported on glass cylinders by a sol–gel technique.

While Fig. 5 overlays dark and photocatalytic inactivation, Fig. 6 shows only inactivation in the dark. A slight impact on bacterial viability can be observed during the first 30 min of the experiment (0.5 log), but after 90 min at 10 L/min, dark inactivation contributes significantly (2 log) to total bacterial reduction. It can also be observed that dark inactivation increases with increasing flow rate. This tendency might be explained by "shear damage" to the bacterial cells from mechanical agitation. Although shear damage has not yet been completely described in solar reactors, the same tendency to bacterial survival in the dark was found by Fernández et al. [23]. Shear damage to different types of cells is most often mentioned in bioprocesses [30–32,46]. There is even literature about shear damage to *E. coli* that reports increasing bacterial inactivation or changes in bacterial physiology with stronger mechanical agitation [34,47]. Bacterial inactivation over the experimental time shows that bacterial resistance weakens with continued mechanical stress.

Opposite tendencies occurring during solar photocatalytic disinfection and in the dark can be explained by the different way in which bacterial viability is affected by mechanical stress (dark) or attack by radicals (sunlight + $TiO_2$). While the mechanical stress slowly but continuously gets stronger with higher flow rates over experimental time, radicals overwhelm bacterial resistance only after a lag phase, which is shorter at slow flow rates, due to better interaction between bacterial cells and photocatalyst.

### 3.4. Influence of initial bacterial concentration on bacterial inactivation

Figs. 7 and 8 show experiments with various initial concentrations at 10 L/min to determine the influence of the initial bacterial concentration on the photocatalytic disinfection and the bacterial viability in the dark. During solar photocatalytic disinfection (Fig. 7), the experiment starting at $10^5$ CFU/mL had a final concentration of 10 CFU/mL, at 4 kJ/L, while the

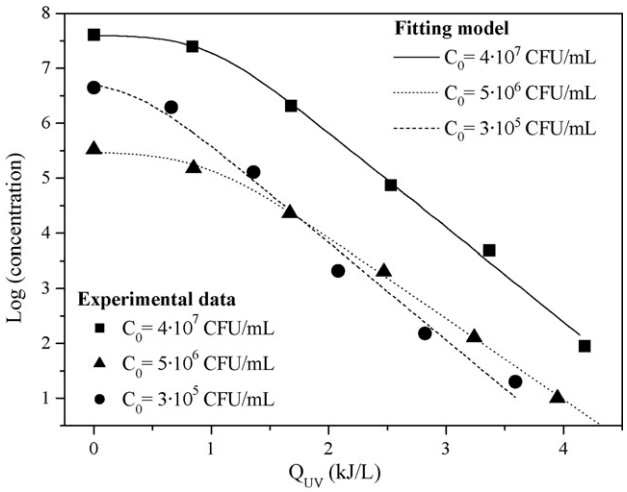


Fig. 7. *E. coli* log concentration in the CPC reactor during solar $TiO_2$ photocatalytic experiments in distilled water at 2 L/min for three initial bacterial concentrations, $4 \times 10^7$ CFU/mL (■), $5 \times 10^6$ CFU/mL (●), and $3 \times 10^5$ CFU/mL (▲).

$10^6$ CFU/mL experiment decreased to 20 CFU/mL at 3.6 kJ/L and the $10^7$ CFU/mL experiment to 90 CFU/mL at 4.2 kJ/L. While there is little difference between the lower concentrations of $10^5$ and $10^6$ CFU/mL, at the highest concentration of $10^7$ CFU/mL, more UV energy is needed for the same disinfection. This tendency to first-order kinetics has been reported previously for disinfection with $TiO_2$ slurries [9,14]. However, when fitted to a logarithmic scale, the disinfection rate is not linear, but has a shoulder at the beginning.

Fig. 7 shows the best fits found by GInaFiT for a log linear regression with shoulder, which has also been reported for most solar bacteria disinfection processes. Its shape depends on the strain and the specific growth rate of bacteria [7,14,42]. In the first step of the solar disinfection treatment, the shoulder effect can be attributed to UV-induced self-defence mechanisms [14]. Our results with the catalyst show a smaller shoulder than those found for solar disinfection in the studies mentioned. The kinetics observed here can be explained by simultaneous solar $TiO_2$ and solar-only disinfection. The fixed catalyst improves the action of sunlight alone, as shown in Fig. 3, but does not reach the fast first-order inactivation reported for $TiO_2$ slurry.

For the dark studies (Fig. 8) the experiment performed at an initial bacterial concentration of $10^6$ CFU/mL shows a 2-log decrease in viability (99%), the one at $10^5$ CFU/mL, a 1-log decrease (95%), and the one at $10^4$ CFU/mL, a 4-log decrease (99.96%). In our experiments, the $10^4$-CFU/mL initial concentration was critical, as the detection limit was reached within 90 min. Higher bacterial concentrations made the influence of dark inactivation less noticeable in the final disinfection results.

Influence of bacterial concentration on its viability in different types of water has also been reported by Kerr et al., who studied *E. coli* viability in distilled water, sterile mineral water and in natural mineral water. Water quality turned out to be less important for bacterial survival at higher bacterial concentrations than at lower [28]. Tailing in the curves in Fig. 8 might be caused by the presence of a part of the bacterial population being more resistant to imposed osmotic and mechanical stress. Such tailing is also observed in disinfection processes, where resistant populations dominate the inactivation rates [9].

### 3.5. Influence of osmotic stress on bacterial viability

To determine any possible effect of osmotic stress on bacterial cells, experiments were performed in the dark with distilled water and a saline solution (0.9 wt.% NaCl) at 2 L/min, because the least mechanical stress was expected at this flow rate. The bacterial concentration most affected, $10^4$ CFU/mL, was chosen as the initial concentration for this experimental series (Fig. 9).

While the bacteria in distilled water decreased 4 log to the detection limit, the concentration in the saline solution

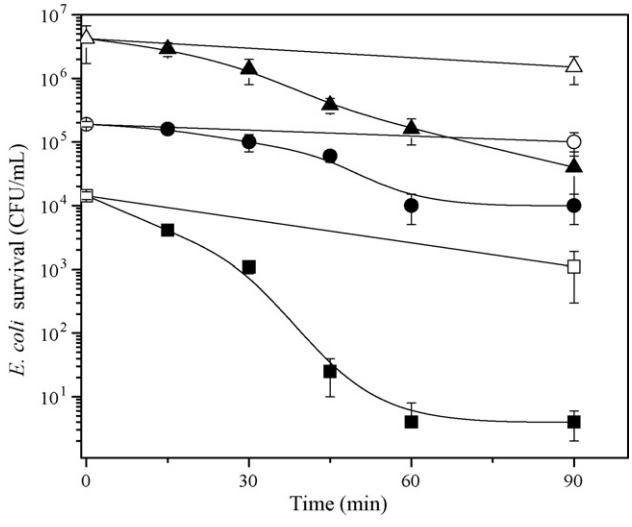


Fig. 8. *E. coli* concentrations in the CPC reactor during three dark runs at various initial bacterial concentrations: $10^4$ CFU/mL (■), $2 \times 10^5$ CFU/mL (●), $4 \times 10^6$ CFU/mL (▲). Open symbols (□, ○, △) represent control samples. Each point represents the average value; the bars show the statistical error at a 95% level of confidence.

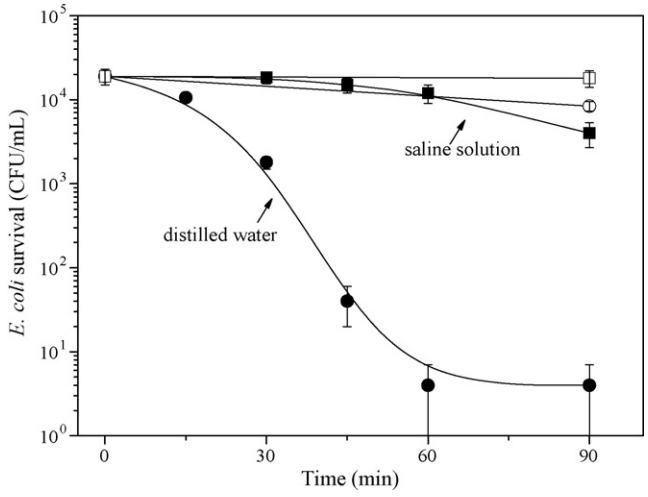


Fig. 9. *E. coli* concentration in the CPC reactor during two dark runs with distilled water (●) and saline solution (■). $C_0 \sim 10^4$ CFU/mL. Flow rate 2 L/min. Open symbols (□, ○) represent the control samples. Each point is an average. The bars show the statistical error at a 95% level of confidence.

decreased less than one log (0.7 log). Such different behaviour shows the effect of mechanical stress with and without osmotic stress. On the other hand, the bacterial concentration in the saline control sample remained stable during the experiment in the dark, while the distilled water control sample showed a 0.4-log decrease in concentration, the same as in all the other experiments performed in distilled water, demonstrating the effect of osmotic stress without any other influence. Thus, mechanical stress alone together with osmotic stress alone would only explain a decrease in viability of approximately 1 log. The fact that our results in distilled water in the dark show significantly higher bacterial inactivation than additional osmotic and mechanical stress alone, can be explained by the influence of mechanical agitation on the bacterial cell osmoregulatory system.

It is commonly accepted that *E. coli* osmolarity, whether osmolarity conditions are high or low, is regulated through mechanosensitive channels [48–52]. These mechanosensitive channels permit bacteria to maintain turgor pressure even under severe changes in osmolarity. In low osmolarity environments, water starts entering the cell due to osmotic pressure, mechanosensitive channels expel ions into the media and turgor pressure consequently decreases. Wase and Patel found a linear increase in cell volume with increasing agitation rates for chemostat-cultivated *E. coli*, which they explain by an increase in water content in the cells [33]. In a later paper, they reported a sharp increase in intracellular ion concentration in *E. coli* as agitation rates increased [34]. These authors give several possible explanations for this, but the reason for the increase in measured ion concentration is not completely clear. Nevertheless, these contributions lead us to expect that mechanical agitation under certain conditions affects the *E. coli* osmoregulatory system. We therefore think that in our case, mechanical stress due to recirculation in the reactors may interfere with the complex osmoregulation of the bacterial cell in distilled water, and therefore causes changes in bacterial resistance during the disinfection process.

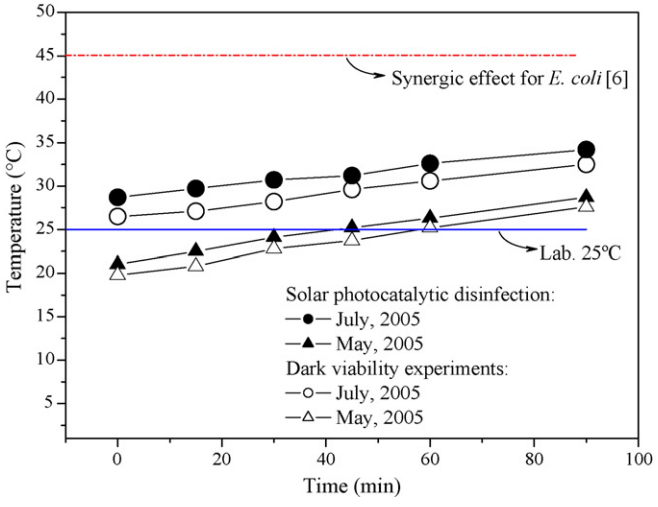


Fig. 10. Temperature in the CPC reactor during solar photocatalytic (●, ▲) and dark experiments (◯, △). Control samples were stored at in the lab 25 °C in the dark (—).

### 3.6. Influence of temperature

Temperature was monitored during all experiments. The temperature profiles of the water in the photoreactor during photocatalytic and dark viability experiments are shown in Fig. 10. The temperature curves shown are the highest and lowest profiles during the experiment series. The highest temperatures were measured in disinfection experiments done in July. This curve shows slightly higher temperatures (approximately 2 °C) than in the dark viability experiments also done in July. The lowest temperatures were found in disinfection and dark experiments done in May. Even the experiments in July did not reach 40 °C, the temperature required for synergy of solar irradiation and temperature [6].

Temperatures were between 19.8 and 32.5 °C in all viability experiments, so that the decrease in bacterial concentration cannot be due to a thermal effect. Nevertheless, increasing cell metabolic activity might increase the response to osmotic stress, and thereby also contribute to increasing bacterial inactivation during the experiment.

## 4. Conclusions

- Using $TiO_2$ immobilized on Ahlstrom paper at concentrations of $10^6$ CFU/mL, photocatalytic disinfection was complete after 90 min in the CPC reactor. The Ahlstrom catalyst thus reduces bacterial concentrations significantly faster than solar disinfection alone.
- Photocatalytic disinfection was found to be more efficient at lower flow rates. This means that low-power pumps should be used for these applications. Such reduced energy consumption is of special interest for rural water disinfection systems operating on a solar power supply.
- Depending on experimental conditions, approximately 99% of bacterial inactivation was shown to be caused by this mechano-osmotic dark inactivation during experiments in solar reactors. Mechanical inactivation increased with rising flow rates and was notably reduced in saline solution (water with NaCl 0.9 wt.%). This phenomenon is of great importance when evaluating the performance of solar photocatalytic disinfection systems (a solar reactor and photocatalyst). Photocatalytic disinfection of distilled water at bacterial concentrations below $10^5$ CFU/mL is caused entirely by mechano-osmotic effects, which, if not taken into account, could be attributed to solar photocatalysis.

## Acknowledgements

This work received funding from the European Union under contract no. 031650-SODISWATER, and from the Spanish Ministry of Education and Science under its Technical and Agrofoods Resources Program (Contract no. AGL2006-12791-C02-01/AGR-FITOSOL). The authors thank Ahlstrom Research & Services for supply of the photocatalyst. They also wish to thank Mrs. Deborah Fuldauer for the English language revision.

## References


[1] Metcalf, Eddy, Wastewater Engineering Treatment and Reuse, fourth ed., Metcalf & Eddy, Inc., 2005.
[2] G. Bitton, Wastewater Microbiology, third ed., John Wiley and Sons, New Jersey, 2005.
[3] W.J. Jarvis, Control de Enfermedades en Cultivos de Invernadero, Ediciones Mundi-prensa, 1998, 333 pp.
[4] T. Joyce, K.G. McGuigan, M. Elmore-Meegan, R. Conroy, Appl. Environ. Microbiol. 62 (1996) 399–402.
[5] K.G. McGuigan, F. Méndez-Hermida, J.A. Castro-Hermida, E. Ares-Mazás, S.C. Kehoe, M. Boyle, C. Sichel, P. Fernández-Ibañez, B.P. Meyer, S. Ramalingham, E.A. Meyer, J. Appl. Microbiol. 101 (2006) 453–463.
[6] K.G. McGuigan, T.M. Joyce, R.M. Conroy, J.B. Gillespie, M. Elmore-Meegan, J. Appl. Microbiol. 84 (1998) 1138–1148.
[7] M. Berney, H.U. Weilenmann, A. Simonetti, T. Egli, J. Appl. Microbiol. 101 (2006) 828–836.
[8] S. Gelover, L.A. Gomez, K. Reyes, M.T. Leal, Water Res. 40 (2006) 3274–3280.
[9] A.G. Rincón, C. Pulgarín, Appl. Catal. B: Environ. 49 (2004) 99–112.
[10] S.C. Kehoe, T.M. Joyce, P. Ibrahim, J.B. Gillespie, R.A. Shahar, K.G. McGuigan, Water. Res. 35 (2001) 1061–1065.
[11] J.M. Herrmann, Top. Catal. 34 (2005) 49–65.
[12] J.R. Hoffmann, S.T. Martin, W.Y. Choi, D.W. Bahnemann, Chem. Rev. 95 (1995) 69–96.
[13] A. Fujishima, T.N. Rao, D.A. Tryk, J. Photochem. Photobiol. C Photochem. Rev. 1 (2000) 1–21.
[14] A.G. Rincón, C. Pulgarín, Appl. Catal. B: Environ. 44 (2003) 263–284.
[15] A.G. Rincón, C. Pulgarín, Sol. Energy 77 (2004) 635–648.
[16] A.G. Rincón, C. Pulgarín, Catal. Today 101 (2005) 331–344.
[17] J. Blanco-Gálvez, P. Fernández-Ibáñez, S. Malato-Rodríguez, J. Solar Energy Eng. Trans. ASME 129 (2007) 1–12.
[18] D.M. Blake, P.C. Maness, Z. Huang, E.J. Wolfrum, J. Huang, J. Sep. Purif. Methods 28 (1999) 1–50.
[19] P.C. Maness, S. Smolinski, D.M. Blake, Z. Huang, E.J. Wolfrum, W.A. Jacoby, Appl. Environ. Microbiol. 65 (1999) 4094–4098.
[20] K. Sunada, T. Watanabe, K. Hashimoto, J. Photochem. Photobiol. A: Chem. 6221 (2003) 1–7.
[21] P. Zhang, R.J. Scrudato, G. Germano, Chemosphere 28 (1994) 607–611.
[22] S.S. Block, V.P. Seng, D.W. Goswami, J. Sol. Energy Eng. 119 (1997) 85–91.
[23] P. Fernández, J. Blanco, C. Sichel, S. Malato, Catal. Today 101 (2005) 345–352.
[24] A. Vidal, A.J. Díaz, A. El Hraiki, M. Romero, I. Muguruza, F. Senhaji, J. González, Catal. Today 54 (1999) 183–290.
[25] A. Vidal, A.J. Díaz, Water Environ. Res. 72 (2000) 271–276.
[26] O.A. McLoughlin, P. Fernández-Ibañez, W. Gernjak, S. Malato Rodríguez, L.W. Gill, Sol. Energy 77 (2004) 625–633.
[27] S. Malato, J. Blanco, A. Vidal, C. Richter, Appl. Catal. B: Environ. 37 (2002) 1–15.
[28] M. Kerr, M. Fitzgerald, J.J. Sheridan, D.A. McDowll, I.S. Blair, J. Appl. Microbiol. 87 (1999) 833–841.
[29] J. Wist, J. Sanabria, C. Dierolf, W. Torres, C. Pulgarin, J. Photochem. Photobiol. A: Chem. 147 (2002) 241–246.
[30] P.S. Cherry, E.T. Papoutsakis, Bioproc. Eng. 1 (1986) 29–42.
[31] A. Handa-Corrigan, A.N. Emery, R.E. Spier, Enzyme Microb. Technol. 11 (1989) 230–235.
[32] Z. Zhang, M.A. Ferencyi, C.R. Thomas, Chem. Eng. Sci. 47 (1992) 1347–1354.
[33] D.A.J. Wase, Y.R. Patel, J. Gen. Microbiol. 131 (1985) 725–736.
[34] D.A.J. Wase, H.A.M. Rattwatte, Appl. Microbiol. Biotech. 22 (1985) 325–385.
[35] M. Collares-Pereira, J. Chaves, J. Correia de Oliveira, Portuguese Patent, 2004.
[36] J. Blanco, S. Malato, P. Fernández-Ibañez, A. Vidal, A. Morales, P. Trincado, J. Oliveira, C. Minero, M. Musci, C. Casalle, M. Brunote, S. Tratzky, N. Dischinger, K.H. Funken, C. Sattler, M. Vincent, M. Collares-Pereira, J.F. Mendes, C.M. Rangel, Sol. Energy 67 (2000) 317–330.
[37] Ahlstrom, EP1069950B1 European Patent, 1999.
[38] C. Guillard, J. Disdier, C. Monnet, J. Dussaud, S. Malato, J. Blanco, M.I. Maldonado, J.M. Herrmann, Appl. Catal. B: Environ. 46 (2003) 319–332.
[39] M. Kositzi, I. Pulios, S. Malato, J. Caceres, A. Campos, Water Res. 38 (2004) 1147–1154.
[40] A.H. Geeraerd, C.H. Herremans, J.F. Van Impe, Int. J. Food Microbiol. 59 (2000) 185–209.
[41] A.H. Geeraerd, V.P. Valdramidis, J.F. Van Impe, Int. J. Food Microbiol. 102 (2005) 95–105.
[42] M. Berney, H. Weilenmann, J. Ihssen, C. Bassin, T. Egli, Appl. Environ. Microbiol. 72 (2006) 2586–2593.
[43] W.D. Bigelow, J.R. Esty, J. Infect. Dis. 27 (1920) 602–617.
[44] P. Mafart, O. Couvert, S. Gaillard, I. Leguerinel, Int. J. Food Microbiol. 72 (2002) 107–113.
[45] O. Cerf, F. Metro, J. Appl. Bacteriol. 42 (1977) 405–415.
[46] C.R. Thomas, in: M.A. Winkler (Ed.), Chemical Engineering Problems in Biotechnology, Elsevier, UK, 1990, pp. 23–94.
[47] C.J. Hewitt, L.A. Boon, A.W.N. McFarlane, The Use of Flow Cytometry to Study the Impact of Fluid Mechnical Stress on *Escherichia coli* W3110 During Continuous Cultivation in an Agitated Bioreactor, John Wiley and Sons, New Jersey, 1998, pp.139–155.
[48] P. Blount, S.I. Sukharev, M.J. Schroeer, S.K. Nagle, C. Kung, Cell Biol. 93 (1996) 11652–11657.
[49] N. Levina, S. Totemeyer, N.R. Stokes, A.M. Jones, I.R. Booth, EMBO J. 18 (1999) 1730–1737.
[50] I.R. Booth, P. Louis, Curr. Opin. Microbiol. 2 (1999) 166–169.
[51] C.P. Biggin, M.S.P. Sansom, Curr. Biol. 13 (2003) 183–185.
[52] G. Calamita, B. Kempf, M. Bonhivers, W.R. Bishai, E. Bremer, P. Agre, Proc. Natl. Acad. Sci. U.S.A. Cell Biol. 95 (1998) 3627–3631.